

Spectroscopic and dynamical studies of the S_1 and S_2 states of decatetraene in supersonic molecular beams

Horioe Petek, Andrew J. Bell, and Keitaro Yoshihara
Institute for Molecular Science, Myodaiji, Okazaki 444, Japan

Ronald L. Christensen
Department of Chemistry, Bowdoin College, Brunswick, Maine 04011

(Received 3 December 1990; accepted 27 June 1991)

Fluorescence and fluorescence excitation spectra of *all-trans*-2,4,6,8-decatetraene have been obtained in free jets and in inert-gas clusters. In isolated decatetraene, excitation into 1^1B_u (S_2) results in emission from both S_2 ($1^1B_u \rightarrow 1^1A_g$) and S_1 ($2^1A_g \rightarrow 1^1A_g$) on time scales

shorter than the 10 ns experimental resolution. In inert-gas clusters, vibrational relaxation leads to long-lived (360 ns) emission from thermally relaxed levels of S_1 . Direct excitation of low-lying, S_1 vibronic levels in cold, isolated molecules also results in long-lived $S_1 \rightarrow S_0$ fluorescence, as expected for this symmetry-forbidden transition. The detection of S_1 emission in free decatetraene has permitted the first detailed study of the vibronic structure and kinetics of the 2^1A_g state of an isolated, *all-trans* linear polyene. The $S_1 \leftarrow S_0$ fluorescence excitation spectrum is rich in low-frequency vibronic progressions. Analysis of this spectrum suggests that the transition not only is made allowed by vibronic coupling involving low-frequency b_u skeletal modes (Herzberg-Teller coupling), as for polyenes in condensed phases, but also gains intensity from interactions between the electronic motion and the hindered

(S_1) state. For isolated decatetraene, the 2^1A_g fluorescence lifetimes show a monotonic decrease with increasing vibrational energy, presumably due to increased mixing with the 1^1B_u state.

I. INTRODUCTION

The low-lying excited states of linear polyenes have been the subject of considerable experimental and theoretical

interest. This interest has been motivated by the roles of polyenes in several important photobiological processes, including energy transfer and photoprotection in photosynthesis and cis-trans photoisomerization in visual systems and photosynthetic bacteria.

Photochemical reactions such as photoinduced cycloadditions and other pericyclic reactions.^{2,3} Experimental work in these areas has been reinforced by a long-standing interest in developing better theoretical descriptions of one-dimensional, conjugated π electron systems. Polyenes provide many examples where the interactions between theory and experiment have led to a deeper understanding of excited-state electronic structures and chemical dynamics.

Much of the recent information about polyene electronic states has come from studies of model systems of intermediate length.⁴⁻¹⁶ Optical experiments on simple polyenes with four or more conjugated double bonds have

revealed the ground state [1^1A_g (S_0)] and first one-photon-allowed excited state [1^1B_u (S_2)].¹ In condensed phases, absorption into the 1^1B_u state is typically followed by a red-shifted

emission from the S_1 state. This emission is sensitive to details of molecular structure and environment. Thus octatetraene and longer polyenes have substantial $S_1 \rightarrow S_0$ fluorescence yields (e.g., $\Phi_f > 0.70$ for *all-trans* octatetraene in rigid glasses and mixed crystals),⁴ whereas hexa-

triene and shorter polyenes have very low yields ($\Phi_f < 10^{-3}$). The lack of emission from shorter polyenes has made it difficult to establish the ordering of their lowest excited states, let alone the details of excited-state relaxation and photochemical pathways in these prototypical systems.

The ordering of the lowest excited states of butadiene and hexatriene and those of the longer polyenes is most likely related to differences in the excited state (2^1A_g and 1^1B_u) geometries of these molecules.^{17,18} Although ethylene undergoes a 90° twist upon excitation from 1^1A_g to 1^1B_u ,¹⁹ theoretical calculations^{20,21} and modeling of resonance Raman and absorption spectra²²⁻²⁵ indicate that the 1^1B_u states of butadiene and longer polyenes retain their planar, ground-state structures. In contrast, *ab initio* calculations on butadiene and hexatriene predict that the low-lying 2^1A_g state is nonplanar.^{17,18} The 2^1A_g state in octatetraene apparently is planar but with a low barrier (~ 1400 cm⁻¹) to cis-trans isomerization.^{26,27} Recent cal-

culations on longer polyenes have shown that the 2^1A_g state is nonplanar and that the 1^1B_u state is planar. The 2^1A_g state is nonplanar due to the presence of low-frequency a_u and b_g symmetry to play important roles in $2^1A_g \rightarrow 1^1A_g$ internal conversion. This is in contrast to the 1^1B_u state which is planar and has a high barrier to isomerization.

quenching of fluorescence. Similar effects should enhance internal conversion from 1^1B_u to 2^1A_g . A nonplanar 2^1A_g state thus should promote the nonradiative relaxation of the initially excited 1^1B_u state by internal conversion. For longer polyenes, more planar 2^1A_g states result in slower rates of $S_1 \rightarrow S_0$ internal conversion, allowing fluorescence to occur.



2,4,6,8-decatetraene

FIG. 1. All-trans-2,4,6,8-decatetraene.

Even though polyenes longer than hexatriene fluoresce, simple model systems have not been extensively studied. This, in part, is due to the fact that they are not commercially available and are difficult to synthesize and purify in the amounts required to carry out extensive vibrational and electronic studies, particularly in molecular beams. Certain natural products, most notably derivatives of the visual chromophore retinal and longer polyenes such as β -carotene, are available and have received a great deal of experimental attention.^{1,16} However, the relative complexity of these systems often prohibits detailed theoretical analysis, and their low vapor pressures have precluded studies under isolated,

short diphenylpolyenes, on the other hand, are both stable and highly fluorescent and thus amenable to detailed spectroscopic and kinetic studies.²⁸⁻⁴⁰ *Cis-* and *trans-*stil-

ed molecules.^{30-32,39-41} These experiments have followed the *cis-trans* photoisomerization on short time scales (10^{-9} – 10^{-13} s) and have provided detailed information on how electronic excitation is directed toward photochemical channels on excited state potential surfaces. Ultrahigh-resolution

of *trans*-stilbene and diphenylbutadiene in molecular beams

chemistry of clusters in supersonic beams also has allowed

in the phenyl-substituted systems.

The forbidden $2^1A_g \leftarrow 1^1A_g$ transition is below the optically

systems thus has much in common with that of unsubstituted analogs. However, the comparison of fluorescence yields reminds us that phenyl substituents have striking effects on the photophysical properties of polyenes, and it would not be surprising if the photochemistries were similarly affected. It thus will be important to extend the experiments on the diphenylpolyenes to unsubstituted polyene systems.

Two recent studies have opened the way to more-detailed experimental investigations of the spectroscopy and photochemistry of the intermediate length, unsubstituted polyenes. Buma, Köhler, and Song⁴³ have used multiphoton

the $2^1A_g \leftarrow 1^1A_g$ transition in several supersonically cooled *cis*-trienes. Extension of these experiments to *trans*-trienes (which have a much weaker $2^1A_g \leftarrow 1^1A_g$ oscillator strength) and dienes would circumvent the problems imposed by the lack of emission in these short chains. Buma and

Bouwman *et al.*⁴⁴ have reported emissions from the S_1

(2^1A_g) and S_2 (1^1B_u) states of several simple tetraenes and pentaenes, both as static gases and in supersonic jets. Previous gas-phase experiments on octatetraene indicated emission solely from the S_2 (1^1B_u) state,^{8,11} while in condensed phases rapid electronic and vibrational relaxation results in emission only from the S_1 (2^1A_g) state.⁵⁻⁸ The discovery of $2^1A_g \rightarrow 1^1A_g$ emissions from isolated polyenes and the development of improved synthetic procedures means that the structures and dynamics of the 2^1A_g states of longer polyenes now can be studied in supersonic expansions with and

without ($2^1A_g \rightarrow 1^1A_g$ and $2^1A_g \rightarrow 1^1A_g$) following excitation of the 1^1B_u state, the one-photon, $2^1A_g \leftarrow 1^1A_g$ fluorescence excitation spectrum, and the single vibronic level

spectroscopy and dynamics of 2^1A_g states in several intermediate-length polyenes.

II. EXPERIMENT

The all-trans-2,4,6,8-decatetraene was prepared by

phenylphosphonium bromide ("Instant Yield", Fluka)

solvent and the solution was stirred for 15 min, 5.5

min the reaction was quenched in a 10% NaOH solution and

mixture was then extracted into warm hexane and allowed

the eluting solvent. Crystalline decatetraene (mp of 137–139 °C) was obtained by precipitation from concentrated hexane solutions. Typical yields after the first recrystallization were > 50%. Crystalline samples stored in sealed vials at -20 °C were stable for several months.

The apparatus for measuring fluorescence excitation and emission spectra of molecules in molecular beams has been

isolated conditions and in clusters has been described previously.⁴⁴ Briefly, the experimental setup consists of (i) a molecular-beam machine, (ii) an excimer-pumped dye laser excitation source, and (iii) emission detection optics and electronics.

A molecular beam of decatetraene was prepared by placing 10–50 mg of all-trans-decatetraene in a trough on the bottom flange next to the orifice of the pulsed molecular-beam valve, heating the sample to 50–80 °C to achieve sufficient vapor pressure.

the 300–400 μ s opening of the nozzle. In some cases higher

higher temperatures. Decatetraene was studied as a free molecule by coexpanding the sample with up to 3000 Torr of He or in Ar clusters by replacing the He carrier gas with up to 3000 Torr of Ar. In He expansions, there was no evidence

However, Ar_n:decatetraene cluster formation occurred above ~300 Torr of Ar stagnation pressure. At higher Ar

The excitation source for fluorescence measurements was an excimer-pumped dye laser (Lambda-Physik 104/2003). The second harmonic of Rhodamine 6G and the fundamental of *p*-terphenyl dye lasers were used to excite the S₂ and S₁ states, respectively. The bandwidth of the dye

and 30 Hz for emission spectroscopy. The excitation intensity was carefully controlled with neutral density filters in case

zle-to-laser beam distance, indicating that at the point of

interaction the sample had reached its terminal temperature measurements. This is crucial due to the long lifetimes of the S₁ state. The focusing of the laser beam was adjusted for excitation of the maximum number of molecules in the observation region, without saturating the transition.

used onto a Hamamatsu Photonics H3177 photomultiplier for fluorescence excitation spectra or onto the slit of a 250 mm monochromator for resolved emission spectra. For

signal was integrated by a Stanford Research Systems boxcar integrator (SR-250), and the integrated value averaged and stored in a microcomputer. Simultaneously, the power of the excitation laser was monitored by a photodiode, whose signal was integrated with another channel of the boxcar, and the output measured to normalize the excitation spectra

by averaging the signal obtained from 10 excitation pulses for each 0.3 cm⁻¹ scan interval.

In order to record emission spectra, the fluorescence

Hz excitation rate.

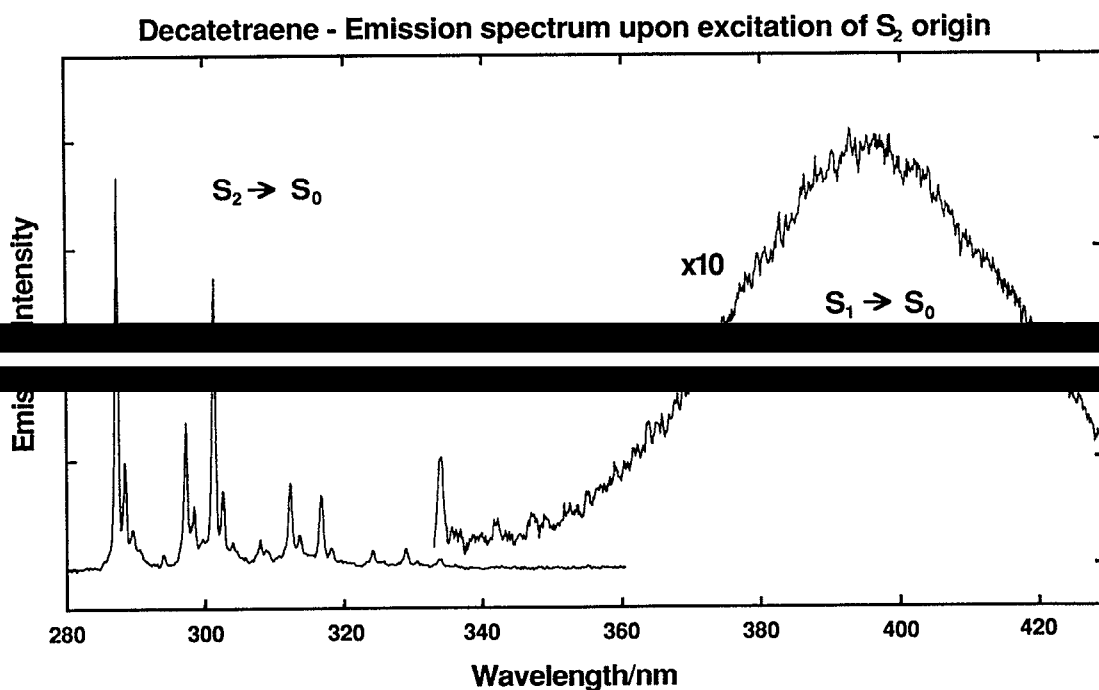


FIG. 2. ${}^1A_g \rightarrow {}^1A_g$ fluorescence of *all-trans*-decatetraene in a free jet following excitation of $1\ {}^1B_u \leftarrow 1\ {}^1A_g$ electronic origin (287.49 nm). (Resolution = 60 cm⁻¹.)

III. RESULTS AND DISCUSSION

A. Dual fluorescence following $S_2 \leftarrow S_0$ excitation of isolated decatetraene

The emission spectrum obtained upon excitation of the $S_2 \leftarrow S_0$ electronic origin (287.49 nm) of isolated, jet-cooled decatetraene is given in Fig. 2. This spectrum reveals two distinct transitions: a well-resolved emission with an electronic origin coincident with the (0-0) of the $S_2 \leftarrow S_0$ absorption, and an unstructured emission at longer wavelengths. The structured fluorescence is assigned to $S_2 \rightarrow S_0$ ($1^1B_u \rightarrow 1^1A_g$) emission from the electronic origin of 1^1B_u . This emission shows a close mirror-image relationship with

ric carbon-carbon single-bond and carbon-carbon double-bond stretches. The relative dominance of the electronic origin indicates that, as with other long polyenes, the

modes, we also observe low-frequency modes at 150 and 290 cm^{-1} which can be assigned to a_g in-plane angle deformations. Similar modes have been observed in the 1^1B_u states

9) and decatetraene (132 and 273 cm^{-1}),¹⁵ though this is been observed for the 1^1A_g state in a free jet.

The broad, unstructured fluorescence previously had been assigned¹⁵ as $S_1 \rightarrow S_0$ ($2^1A_g \rightarrow 1^1A_g$) emission from highly vibrationally excited states of S_1 that are isoenergetic and strongly coupled with the zero-point vibrational level of

The displacement of the Franck-Condon maximum from the origin can be ascribed to differences in the C-C and C=C bond lengths in the 2^1A_g and 1^1A_g states.

to be independent of the laser power, nozzle temperature, He stagnation pressure, and the distance between the nozzle and the point where the laser intersects the molecular beam. In addition, identical $S_2 \leftarrow S_0$ fluorescence excitation spectra were obtained when separately monitoring the two emissions. We thus must conclude that both emissions are from isolated decatetraenes excited to S_2 vibronic states, and in particular that the broad emission is not due to the formation of dimers or excimers in the molecular beam, nor due to absorption to spectroscopically distinct S_2 and S_1 vibronic states.

These results support our previous interpretation of the dual emissions observed in room-temperature, static gas samples of decatetraene and several other polyenes.¹⁵ The ratio of the two emissions in the free jet is comparable to that observed for the static, room-temperature gas ($S_1 \rightarrow S_0/S_2 \rightarrow S_0 = 0.7 \pm 0.2$).¹⁵ This is somewhat surprising given the rather different S_2 vibronic states accessed in the jet and static vapor experiments, but consistent with the observation of identical $S_2 \leftarrow S_0$ excitation spectra when monitoring either S_2 or S_1 emission. Preliminary measure-

ments of lifetimes indicate < 10 ns decay times for both emissions. The $S_2 \leftarrow S_0$ vibronic linewidths have been used to estimate a 0.25 ps lifetime for the zero point level of 1^1B_u .¹⁵ This suggests $< 10^{-4}$ fluorescence yields for both 1^1B_u and 2^1A_g which is not unexpected given the 5762 cm^{-1} of excess energy (the $S_2 - S_1$ energy difference) in the initially excit-

yields await further study.

B. Fluorescence following $S_2 \leftarrow S_0$ excitation of decatetraene/Ar clusters

we have also studied the fluorescence excitation and fluorescence excitation spectra shift to the red with increas-

stagnation pressures of argon (~ 2 atm), complete solvation of decatetraene in large Ar clusters results in rapid electronic

those obtained in low-temperature glasses.⁷ The Franck-Condon envelopes of these spectra correspond well with the broad, red-shifted emission observed for isolated molecules and had further support from the observation of identical

sufficient vibronic detail to allow the assignment of the elec-

forbidden transitions, the corresponding solvent shifts of the $S_1 \leftrightarrow S_0$ spectra are considerably smaller than for the $S_2 \leftrightarrow S_0$ transitions.^{1,12}

Spectra obtained at lower argon pressures show dual emissions, indicating partitioning between complexed and

grows progressively stronger. This suggests that the fluorescence excitation spectra are dominated by the more fluores-

Decatetraene $S_1 \rightarrow S_0$ Emission Spectrum in Ar Clusters

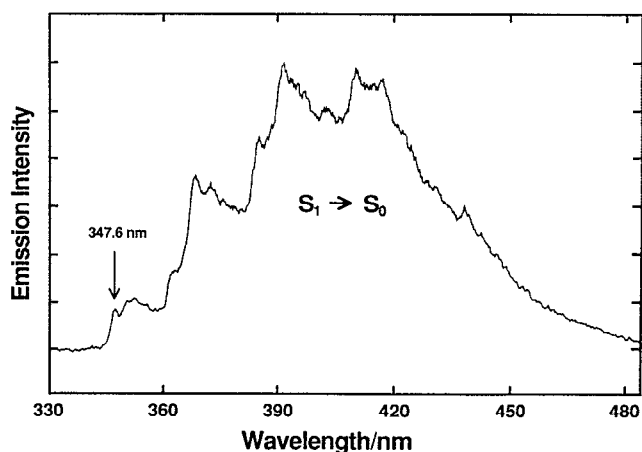


FIG. 3. $2^1A_g \rightarrow 1^1A_g$ fluorescence of *all-trans*-decatetraene in argon clusters following $S_0 \rightarrow S_2$ ($1^1A_g \leftarrow 1^1B_u$) excitation. (Instrumental resolution = 30 cm^{-1} .)

cent, clustered species and that these clusters (along with emission spectra. For larger clusters, decatetraene relaxation is complete and the effective temperature is lower, resulting in the increased resolution of the $S_1 \rightarrow S_0$ emission at high argon pressures (> 2 atm). The $S_1 \rightarrow S_0$ fluorescence lifetimes also are sensitive to cluster size with lower pressures of argon giving shorter, nonexponential decay times. The broader $S_1 \rightarrow S_0$ fluorescence spectra indicate that these

small that $S_1 \rightarrow S_1$ relaxation results in significant heating of traps has fully vibrationally relaxed. These experiments in emissions can be controlled by the argon/decatetraene stoichiometry and that several argons are required to relax the excited decatetraene into the zero-point vibrational level of

($P > 2$ atm) where the decatetraene fluorescence appears is well described by single-exponential kinetics with a decay time of 360 ns. This, the longest emission lifetime observed in

a linear polyene, confirms that the fluorescence is symmetry *all-trans* polyene (*cis* isomer impurities would have considerably shorter S_1 lifetimes due to loss of the inversion center). Previous measurements⁵ of fluorescence lifetimes and quantum yields of *all-trans*-decatetraene in isopentane at room temperature ($\tau_f = 5$ ns, $\phi_f = 0.01$) and at 77 K ($\tau_f = 100$ ns, $\phi_f = 0.2$) indicate an intrinsic radiative lifetime of ~ 500 ns. Comparison between solution, cluster, and

(and expected differences in intensity borrowing through the long, the 260 ns lifetime suggests a large fluorescence yield isolated decatetraene

the vibronic levels of this transition is given in Fig. 5. The complicated development of low-frequency vibronic bands, particularly the splitting of most bands into triplets. The free-jet

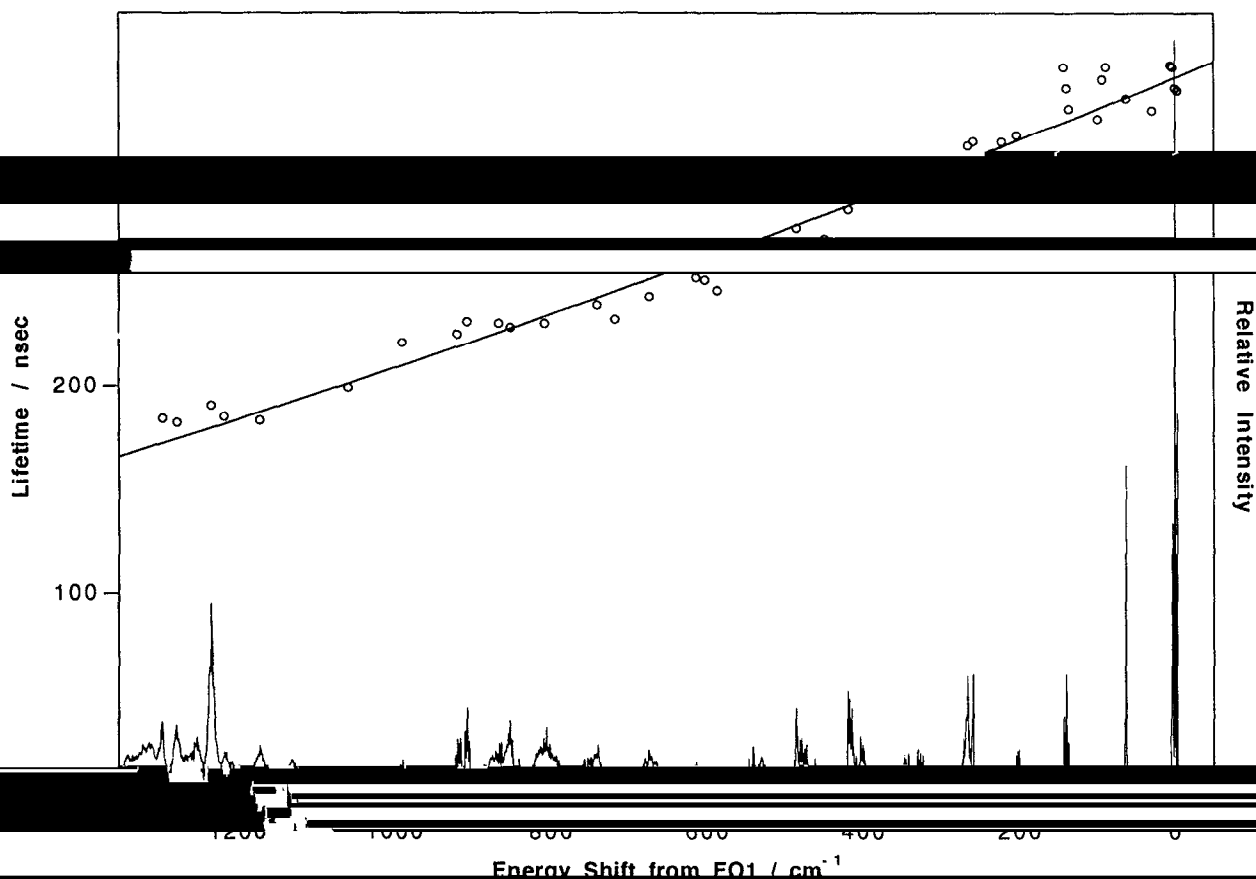


FIG. 4. $214 \rightarrow 114$ fluorescence excitation spectrum and single vibronic level fluorescence lifetimes of *all-trans*-decatetraene in a free jet (0.1350 cm^{-1}).

transitions are dominated by combinations of high-frequency, carbon-carbon stretching modes.^{1,6,7,13,14} Tentative assignments of the most prominent, low-energy $S_1 \leftarrow S_0$ vibronic features are provided in Table I. Also included in this table are the fluorescence lifetimes of most of the vibronic

transitions. Under conditions (site symmetries) that preserve the g and u symmetry labels, polyene $2^1A_g \leftrightarrow 1^1A_g$ spectra exhibit the classic patterns of Herzberg-Teller vibronic coupling. The spectra are characterized by forbidden origins with spectral intensi-

try-forbidden nature of the transition which requires that vibronic intensity be built on "false" origins. Analysis of the $S_1 \leftarrow S_0$ absorption in decatetraene thus rests on the correct

previous work on the fluorescence excitation spectra of decatetraene in 4.2 K n -undecane leads to the identification of a 72 cm^{-1} Herzberg-Teller promoting mode in the 2^1A_g state.⁵

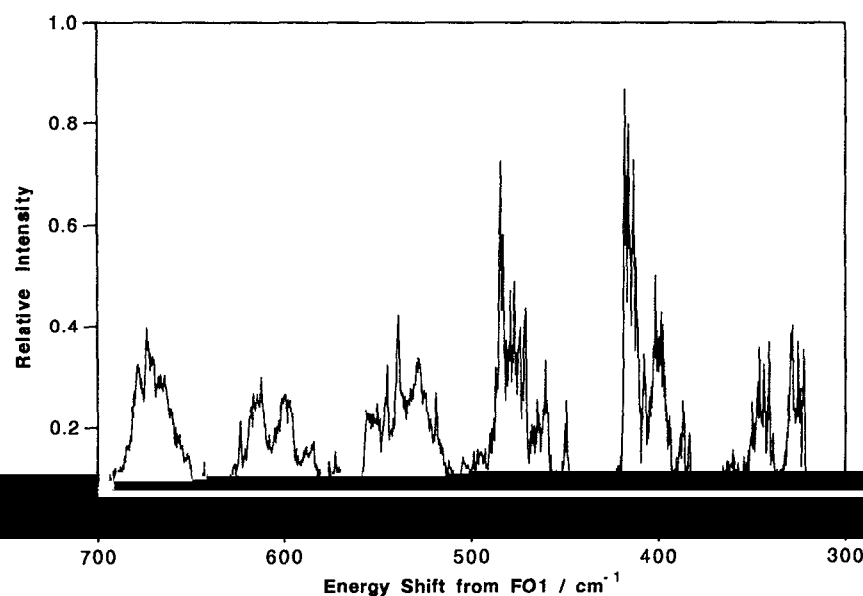
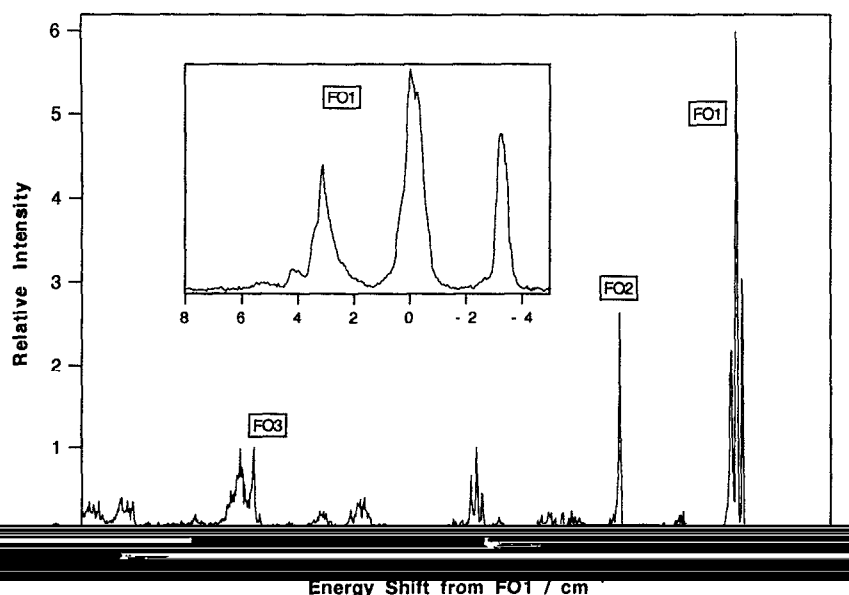


FIG. 5. Expanded views of low-energy vibronic transitions in the $2^1A_g - 1^1A_g$ fluorescence excitation spectrum of *all-trans*-decatetraene in a free jet. Note that the expanded intensity scales of the lower panels. The inset gives an expanded view of false origin 1 (FO1) at a stagnation pressure of 4000 Torr helium and a laser step size of 0.04 cm^{-1} .

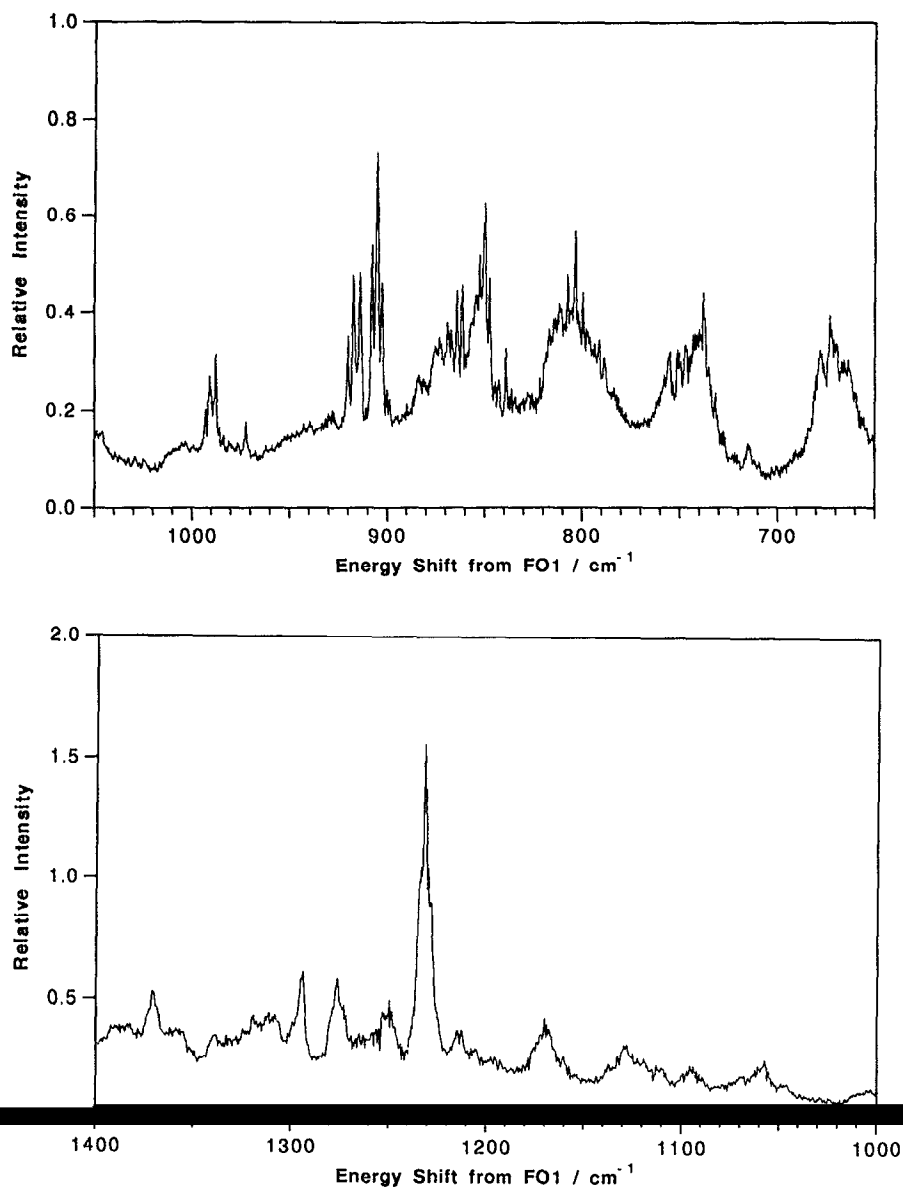


FIG. 5. (Continued).

identify the low-frequency vibrations as b_u in-plane skeletal modes of the polyene chain.⁴⁷⁻⁴⁹ The analysis of the excitation spectrum of isolated decatetraene indicates an analogous false origin system ($\nu = 65$ cm⁻¹) that is identified as false origin 2 (FO2) in Table 1. This mode plays an important (though by no means dominant) role in the low-frequency vibronic development of the $2^1A_g \rightarrow 1^1A_g$

transitions built on FO2 typically appear as sharp, well-defined "singlets." Our inability to observe the symmetry-forbidden electronic origin (0-0) precludes a more-accurate measurement of the frequency of this vibration, though, as will be seen below, there are reasons to estimate an upper bound of 70 cm⁻¹, in good agreement with the b_u

mode observed in the decatetraene/undecane mixed crystal.³

Assignment of the other major false origin system (false origin 1; FO1 in Table 1) for isolated decatetraene is not as straightforward. The lowest energy feature in the $2^1A_g \rightarrow 1^1A_g$ excitation spectrum consists of a triplet of peaks at 29 019, 29 022, and 29 025 cm⁻¹ with the triplet showing indications of additional fine structure (see inset of

not be fully resolved in our experiment (due to a limiting resolution of 0.3 cm⁻¹) and most likely is due to rotational P and R branch envelopes. We have identified the low-energy triplet of peaks (the strongest bands in our spectrum) as a false origin that is induced by coupling between the electronic motion and the hindered rotation of the terminal

TABLE I. Band maxima in the free-jet $2^1A_g \leftarrow 1^1A_g$ fluorescence excitation spectrum of *all-trans*-2,4,6,8-decatetraene.

Frequency (cm ⁻¹) ^a	Assignment	Lifetime (ns)
0 (29 022 cm ⁻¹) (<i>b_u</i>) ^b	FO1	344
63 (<i>b_u</i>)	FO2	339
139 (<i>a_g</i>)	FO1 + 139	344
203 (<i>a_g</i>)	FO1 + 203	321
223 (<i>a_g</i>)	FO1 + 223	318
259 (<i>b_u</i>)	FO3	318
266	FO2 + 203	316
329 (<i>a_g</i>)	FO1 + 329 (FO2 + 266)	301
342	FO1 + 139 + 203	298
387	FO2 + 329	292
400	FO3 + 139	290
416 (<i>a_g</i>)	FO1 + 416	285
461	FO3 + 203	271
474	FO2 + 416	269
484 ^c	FO1 + 2(139) + 203/FO3 + 223	276
529 ^c	FO1 + 203 + 329	260
539 ^c	FO3 + 2(139)/FO1 + 139 + 2(203)	261
601 ^c	FO3 + 139 + 203	251
613 ^c	FO3 + 139 + 223/FO1 + 203 + 416	252
673 ^c	FO1 + 2(139) + 2(203)/FO3 + 3(139) (FO2 + 203 + 416)	243
740 ^c	FO1 + 139 + 3(203)/FO3 + 2(139)/ FO1 + 329 + 416	239
804 (<i>a_g</i>)	FO1 + 804	230
	(FO2 + 139 + 203 + 416)	
850 (<i>a_g</i>)	FO1 + 850	228
852 ^c	FO1 + 2(139) + 3(203)/FO3 + 3(139) + 203	
905 (<i>a_g</i>)	FO1 + 905	231
988 (<i>b_u</i> ?)	FO4(?)	221
1232 (<i>a_g</i> , C=C)	FO1 + 1232	190
1294	FO2 + 1232	184

^bDenotes symmetry of vibrations, assuming that 2^1A_g is described by the C_{2v} point group. As noted in the text.

^a*a_g* or *b_g*.

^cThese bands are broad and most likely are due to the overlap of two or more of the combination bands indicated in the table.

methyl groups. Such couplings have not previously been invoked in discussions of polyene spectra. However, there is ample precedence for this effect in the supersonic jet spectra of several methyl-substituted benzenes⁵⁰⁻⁵³ and fluorotoluenes.⁵⁴ The spectra of these molecules are characterized

the $S_1 \leftrightarrow S_0$ electronic origins, that can be assigned to transitions associated with the internal rotation of the ring methyl groups. Furthermore, these spectra can be accounted for quantitatively by changes in the barriers to rotation in going from the ground to excited electronic states.^{53,54} Of particular interest are the experiments of Ito and co-workers on the electronic spectroscopy of jet-cooled 1,3,5-trimethylbenzene (mesitylene).^{50,51} Mesitylene, like decatetraene, has a symmetry-forbidden $S_1 \leftarrow S_0$ transition and the 0-0 band thus does not appear in the spectrum. A triplet of low-frequency bands appears on the high-energy side of the forbidden 0-0, suggesting strong coupling between the electronic motion

and methyl internal rotation. Totally symmetric vibrations form progressions on the low-frequency triplet as well as on a second, vibronically induced (Herzberg-Teller coupling) false origin for which a single, sharp peak is observed. The true origin of bands in the electronic spectra of mesitylene is assigned to the two false origins in isolated decatetraene.

The appearance of methyl torsional fine structure in the free-jet spectra of substituted benzenes is due to the modest barriers to internal rotation in the ground and excited states of these systems.^{53,54} Indeed, in molecules such as toluene where methyl groups are bonded to a framework of twofold symmetry, the energy levels associated with rotation are essentially those of a free rotor.⁵⁵ This gives rise to the extended (10-200 cm⁻¹) methyl torsional structure seen in the free-jet $S_1 \leftarrow S_0$ spectra of the methyl-substituted benzenes.⁵⁰⁻⁵³ In decatetraene, we also observe some complex clumps of weak transitions within 100 cm⁻¹ of FO1. These

also may be associated with methyl torsions. However, the and predicted at 282 cm^{-1} in ground-state decapentaene⁴⁷

tion. The resulting ground-state tunneling splittings thus are too small to detect in our experiments. The appearance of fine structure in the $S_1 \leftarrow S_0$ transition of decatetraene would require a reduction of the rotational barriers in the 2^1A_g

A significant reduction in the barrier to methyl rotation of the following: (i) *Decreased repulsions between the π -*

tals on the terminal C=C bonds ($\pi_{C=C}$) due to the predicted bond-order inversion between C=C and C-C bonds in going from the ground state to 2^1A_g . Such rearrangements are predicted by theory^{49,59-62} and are indicated by the extended Franck-Condon envelopes seen in the

attractive interactions between the vacant n_{CH_3} and $n_{C=C}$ orbitals.⁶³ If the fine structure seen in the $S_1 \leftarrow S_0$ excitation spectrum is due to hindered rotation, then the electronic origin (0, 0) must lie within a few cm^{-1} of the lowest energy

bronic energy in 2^1A_g (see Table I). It should be stressed, however, that the precise location of the electronic origin has not been determined at this time.

Another possibility to consider is that the triplet of peaks centered at $29\,022\text{ cm}^{-1}$ is due to a second b_u Herzberg-Teller promoting vibration that is merely modulated by the methyl rotations. However, previous experiments and

identified in the $2^1A_g \leftarrow 1^1A_g$ mixed-crystal spectrum of octatetraene.⁴⁶ These frequencies are reasonably well accounted for by theory,⁴⁷⁻⁴⁹ which predicts corresponding modes at lower frequency in molecules such as decapentaene (62, 282, 497, and 553 cm^{-1} in 1^1A_g) and decatetraene.⁴⁷ It thus would be difficult to rationalize two b_u promoting vibrations separated by 63 cm^{-1} , since one of these must be the counterpart of the lowest-frequency b_u modes that play such dominant, well-documented roles in the condensed phase, $2^1A_g \leftarrow 1^1A_g$ transition of ground-state decatetraene (Fig. 1).

and FO2 (see Table I) confirm that they belong to the same transition of the same molecule and that they cannot be due to different conformers or isomers of decatetraene.

Further analysis of the spectrum suggests that the peak 259 cm^{-1} above FO1 should be assigned to a second Herzberg-Teller false origin (FO3). This (like FO2) appears as a single, sharp peak and thus cannot be easily reconciled with an a_g vibration built on the FO1 triplet. This most likely is a

Analysis of the remainder of the $2^1A_g \leftarrow 1^1A_g$ excitation spectrum primarily rests on numerology and the characteristic triplet and singlet structure of progressions built on the two types of false origins. In order to simplify the present

plets" is given in Table I. We first focus on the low-energy (139–203 cm^{-1}) triplet and singlet progressions, and then on the prominent, low-frequency vibronic features seen in Figs.

ing frequencies: 139, 203, 223, 329, and 416 cm^{-1} . The fact that these frequencies appear both as single and double quanta indicates a_g symmetries for these vibrations. (This analysis assumes that decatetraene retains its C_{2h} symmetry in the 2^1A_g state.) However, normal-mode calculations sug-

(a_u or b_g). Two of these modes are most likely the 2^1A_g counterparts of the a_g vibrations that are active in the $1^1B_u \leftarrow 1^1A_g$ absorption (132 and 273 cm^{-1}) (Ref. 15) and

and Rice⁴⁷ predict a_g in-plane bends of 158 and 299 cm^{-1}

tions we have observed for isolated decatetraene. (Decapentaene and decatetraene should have comparable low-frequency, skeletal bending modes due to similar reduced masses and force constants.) However, the next a_g vibration is calculated at 425 cm^{-1} (535 cm^{-1} in octatetraene).⁴⁷⁻⁴⁹ This strongly implies that at least two of the low-frequency vibrations given above involve nontotally symmetric vibrations. There are several low-frequency a_g and b_u candidates

many of the low-frequency a_g and b_u modes) awaits calculation of the decatetraene 1^1A_g and 2^1A_g normal modes.

It should be stressed that the analysis given in Table I uses the *minimum* number of low-frequency modes to account for the bulk of the $S_1 \leftarrow S_0$ excitation vibronic intensity. The triplet fine structure of progressions built on FO1, the number of low-frequency modes, and the approximate coincidence between $FO1 + 203\text{ cm}^{-1}$ and $FO2 + 139\text{ cm}^{-1}$ contribute to a rather complex spectrum. The combination bands of the modes listed in Fig. 5 (low cm^{-1}) modes that could not easily be distinguished from combination bands of the modes listed above. These modes would add to the list of low-frequency, nontotally symmetric vibrations that are active in the spectrum.

Finally, we consider vibronic bands 800 – 1350 cm^{-1} above the $2^1A_g \leftarrow 1^1A_g$ origin. As shown in Figs. 4 and 5, there are several sharp features in the spectrum that are most likely assigned to fundamental. Methyl twisting modes

though it is not possible to make specific assignments at present. The fluorescence lifetimes of the vibronic levels are listed in Table I and plotted in Fig. 4. Lifetimes of the false origins are comparable to those obtained for vibrationally relaxed molecules in argon clusters (~ 360 ns) and again indicate both relatively strong and weak, symmetry-forbidden transitions, as expected for *all-trans*-decatetraene. The relatively smooth falloff in lifetimes further indicates that all of these vibronic features are associated with the same electronic transition and eliminates the possibility that some parts of the spectrum might be assigned to conformers or isomers without inversion centers.

Fluorescence lifetimes for individual vibronic levels are listed in Table I and plotted in Fig. 4. Lifetimes of the false origins are comparable to those obtained for vibrationally relaxed molecules in argon clusters (~ 360 ns) and again indicate both relatively strong and weak, symmetry-forbidden transitions, as expected for *all-trans*-decatetraene. The relatively smooth falloff in lifetimes further indicates that all of these vibronic features are associated with the same electronic transition and eliminates the possibility that some parts of the spectrum might be assigned to conformers or isomers without inversion centers.

Fluorescence lifetimes for individual vibronic levels are listed in Table I and plotted in Fig. 4. Lifetimes of the false origins are comparable to those obtained for vibrationally relaxed molecules in argon clusters (~ 360 ns) and again indicate both relatively strong and weak, symmetry-forbidden transitions, as expected for *all-trans*-decatetraene. The relatively smooth falloff in lifetimes further indicates that all of these vibronic features are associated with the same electronic transition and eliminates the possibility that some parts of the spectrum might be assigned to conformers or isomers without inversion centers.

Fluorescence lifetimes for individual vibronic levels are listed in Table I and plotted in Fig. 4. Lifetimes of the false origins are comparable to those obtained for vibrationally relaxed molecules in argon clusters (~ 360 ns) and again indicate both relatively strong and weak, symmetry-forbidden transitions, as expected for *all-trans*-decatetraene. The relatively smooth falloff in lifetimes further indicates that all of these vibronic features are associated with the same electronic transition and eliminates the possibility that some parts of the spectrum might be assigned to conformers or isomers without inversion centers.

Fluorescence lifetimes for individual vibronic levels are listed in Table I and plotted in Fig. 4. Lifetimes of the false origins are comparable to those obtained for vibrationally relaxed molecules in argon clusters (~ 360 ns) and again indicate both relatively strong and weak, symmetry-forbidden transitions, as expected for *all-trans*-decatetraene. The relatively smooth falloff in lifetimes further indicates that all of these vibronic features are associated with the same electronic transition and eliminates the possibility that some parts of the spectrum might be assigned to conformers or isomers without inversion centers.

$S_2 - S_1$ energy difference decreases. Intensity borrowing documented for polyenes in solution^{1,64} and has been used

phenylbutadiene and diphenylhexatriene in supersonic expansions.^{28,29} The absorption strength of the $2^1A_g \leftarrow 1^1A_g$ transition thus should increase inversely with the square of the energy separation (ΔE) between the 2^1A_g and 1^1B_u states. As seen in Fig. 4, the 2^1A_g vibronic lifetimes of decatetraene are well accounted for by this simple model

The fit indicated in Fig. 4 gives a Γ of $7.6 \times 10^{13} \text{ cm}^{-2} \text{ s}^{-1}$

solvent-dependent lifetimes of diphenylhexatriene and *all-*

of 1.00 and taking an average frequency of the $2^1A_g \leftarrow 1^1A_g$ transition as $29\,000 \text{ cm}^{-1}$ yields a vibronic coupling matrix element of $1.0 \times 10^{-1} \text{ eV}$. (Compare 0.05 and 1.0 eV in diphenylhexatriene and retinol.⁶⁴)

Considering the above arguments, it perhaps is surprising that the free molecule and Ar cluster lifetimes are so

clusters (4300 cm^{-1} vs 5800 cm^{-1} for the free molecule) should almost double the fluorescence decay rate. The comparable fluorescence lifetimes of the clusters and isolated decatetraene is most likely due to higher fluorescence yields in the clusters. This is not unexpected given the expected

sensitivity of nonradiative decay rates on the solvent envi-

less than unity, which might help explain the difference between the ~ 340 ns free-molecule lifetime and the 500 ns lifetime predicted from lifetimes and quantum yield.

IV. SUMMARY AND CONCLUSION

The discovery of $1^1B_u \rightarrow 1^1A_g$ and $2^1A_g \rightarrow 1^1A_g$ emis-

investigated using fluorescence excitation techniques. Mea-

The ability of polyenes to undergo large-amplitude motions is reflected in the important roles played by low-frequency vibrations in the electronic spectra. This is particularly evident in the weak, symmetry-forbidden $2^1A_g \leftarrow 1^1A_g$ transi-

tion which is dominated by progressions of low-frequency modes. Normal coordinate calculations indicate that some of these low-frequency vibrations may involve out-of-plane modes (a_u and b_g) which involve carbon-carbon torsion internal coordinates. Such modes are of obvious interest in understanding the *trans* \leftrightarrow *cis* photochemistries of polyene systems. The low-frequency progressions and doublet of false origins that can, in turn, be assigned to low-frequency (~ 65

and 1^1B_u states. In addition, it appears that the torsional and rocking motions of the terminal methyl groups also are

cally induced, $2^1A_g \rightarrow 1^1A_g$ transition of an *all-trans* polyene.

The flexibility of polyenes distinguishes them from aromatic systems and clearly is an important factor in their unique ground- and excited-state chemistries. However, the important role of large-amplitude motions has not previous-

in solutions and crystals where lattice and phonon modes

connection between methyl torsions and the coupling be-

spectroscopy, though there is precedence for this observation in the spectroscopy of small molecules and in

ty,⁶⁵ and in several methyl-substituted benzenes. Cou-

pling of the methyl torsions to carbon-carbon torsions and other low-frequency modes appears to be strong and perhaps plays an important role in accelerating *cis-trans* isomeriza-

The free-jet, two-photon, $S_0 \rightarrow S_1$ fluorescence excitation spectrum and $S_1 \rightarrow S_0$ fluorescence spectra from single vibronic levels of 2^1A_g would be useful in confirming our spectral assignments as well as providing insights on the role of intramolecular vibrational redistribution (IVR) in these

systems. Extension of our experiments to nonatetraene and octatetraene is in progress and should lead to a better understanding of the role of substituents and the effect of reduced symmetry on the spectroscopy and dynamics of these molecules. The increase in the ratio of $S_1 \rightarrow S_0/S_2 \rightarrow S_0$ fluorescence intensities in gaseous pentaenes indicates that fluorescence and fluorescence excitation techniques should allow similarly detailed studies of the 2^1A_g states of longer polyenes in gas phase and in solvent clusters.

The free-jet experiments described in this paper also

catetraene, nonatetraene, and related molecules would greatly facilitate the analysis of the vibronic spectra and lead to a better understanding of the low-frequency vibrations. Estimates of barriers to internal rotation and cis-trans isomerization in the ground and excited states of these molecules also are of considerable interest. The apparently strong interactions between the π electrons and the methyl rotations clearly deserve further study. Any accounting of the triplet pattern observed for the S_1 origin (Fig. 5) will require a careful study of the methyl rotation. The distinctive structure and splittings of these peaks should provide useful benchmarks for evaluating theoretical descriptions of the 2^1A_g states in model polyenes.

We acknowledge the donors of the Petroleum Research Fund, administered by the American Chemical Society, and a DuPont Fund grant to Bowdoin College, for support of Education, Science and Culture (MONBUSHO) for supporting his initial visit to the Institute for Molecular Science. A.J.B. acknowledges the Japan Society for the Promotion of Science for post-doctoral funding. We thank J. Diener and B. Tounge for synthesizing decatetraene; H. Okamoto for

- ¹¹ L. A. Heimbrook, B. E. Kohler, and I. J. Levy, *J. Chem. Phys.* **81**, 1592 (1984).
¹² R. B. Woodward and R. Hoffman, *The Conservation of Orbital Symmetry*, Prentice-Hall, Englewood Cliffs, NJ, 1973.
¹³ R. M. Gavin, Jr., C. Weisman, J. K. McVey, and S. A. Rice, *J. Chem. Phys.* **68**, 522 (1978).
¹⁴ B. Kohler, C. Spangler, and C. J. Westerfield, *J. Chem. Phys.* **89**, 5422 (1988).
¹⁵ W. G. Bouwman, A. C. Jones, D. Phillips, P. Thibodeau, C. Friel, and R. L. Christensen, *J. Phys. Chem.* **94**, 7429 (1990).
¹⁶ A. G. S. F. de G. and G. W. Scott, *J. Phys. Chem.* **94**, 8118 (1990).
¹⁷ F. Zerbetto and M. Z. Zgierski, *J. Chem. Phys.* **93**, 1235 (1990).
¹⁸ M. Aoyagi, Y. Osamura, and S. Iwata, *J. Chem. Phys.* **83**, 1140 (1985).

- ¹⁹ D. L. Komel, M. A. Spigiani, J. Chem. Phys. **66**, 2405 (1977).
²⁰ J. A. Syage, P. M. Felker, and A. H. Zewail, *J. Chem. Phys.* **81**, 4685 (1984).
²¹ G. J. Dormans, G. C. Groenenboom, and H. M. Buck, *J. Chem. Phys.* **86**, 4895 (1987).
²² A. B. Myers and K. S. Pranata, *J. Phys. Chem.* **93**, 5079 (1989).
²³ M. O. Trulson and R. A. Mathies, *J. Chem. Phys.* **94**, 5741 (1990).
²⁴ R. R. Chadwick, D. P. Gerrity, and B. S. Hudson, *Chem. Phys. Lett.* **115**, 24 (1985).
²⁵ M. F. Granville, G. R. Holtom, and B. E. Kohler, *Proc. Natl. Acad. Sci. U.S.A.* **77**, 31 (1980).

- ²⁶ D. L. Komel and I. A. Spigiani, *J. Chem. Phys.* **66**, 2405 (1977).
²⁷ J. A. Syage, P. M. Felker, and A. H. Zewail, *J. Chem. Phys.* **81**, 4685 (1984).
²⁸ J. A. Syage, P. M. Felker, and A. H. Zewail, *J. Chem. Phys.* **81**, 4706 (1984).
²⁹ A. Amirav and J. Jortner, *Chem. Phys. Lett.* **95**, 295 (1983).
³⁰ J. Troe, A. Amirav, and J. Jortner, *Chem. Phys. Lett.* **115**, 245 (1985).
³¹ A. Amirav, M. Szwarc, and J. Jortner, *Chem. Phys. Lett.* **103**, 9 (1983).

- ³² J. F. Shepanski, B. W. Keelan, and A. H. Zewail, *Chem. Phys. Lett.* **103**, 9 (1983).
³³ T. Itoh and B. E. Kohler, *J. Phys. Chem.* **92**, 1807 (1988).
³⁴ H. Petek, Y. Fujiwara, D. Kim, and K. Yoshihara, *J. Am. Chem. Soc.* **110**, 6269 (1988).
³⁵ J. H. Frederick, Y. Fujiwara, J. H. Penn, K. Yoshihara, and H. Petek, *J. Phys. Chem.* **95**, 2845 (1991).
³⁶ J. F. Pfanstiel, B. B. Champagne, W. A. Majewski, D. F. Plusquellic, and van Harpen and W. I. Maerte, *J. Phys. Chem.* **94**, 6 (1990).

- ¹ B. S. Hudson, B. E. Kohler, and K. Schulten, in *Excited States*, edited by E. C. Lim (Academic, New York, 1982), Vol. 6, p. 1.
² R. B. Woodward and R. Hoffman, *The Conservation of Orbital Symmetry*, Prentice-Hall, Englewood Cliffs, NJ, 1973.
³ R. M. Gavin, Jr., C. Weisman, J. K. McVey, and S. A. Rice, *J. Chem. Phys.* **68**, 522 (1978).
⁴ J. R. Andrews and B. S. Hudson, *Chem. Phys. Lett.* **57**, 600 (1978).
⁵ M. F. Granville, G. R. Holtom, B. E. Kohler, R. L. Christensen, and D'Amico, *J. Chem. Phys.* **70**, 593 (1979).
⁶ K. L. D'Amico, C. Manos, and R. L. Christensen, *J. Am. Chem. Soc.* **102**, 1777 (1980).
⁷ L. A. Heimbrook, I. F. Kenny, B. E. Kohler, and G. W. Scott, *J. Chem. Phys.* **75**, 4338 (1981).
⁸ D. G. Leopold, V. Vaida, and M. F. Granville, *J. Chem. Phys.* **81**, 4210 (1984).
⁹ D. G. Leopold, R. D. Pendley, J. L. Roebber, R. J. Hemley, and V. J. Vaida, *Chem. Phys.* **81**, 4219 (1984).

- ³⁷ R. Howell, H. Petek, D. Phillips, and K. Yoshihara, *Chem. Phys. Lett.* (submitted).
³⁸ R. L. Christensen and B. E. Kohler, *J. Chem. Phys.* **63**, 1837 (1975).
³⁹ M. F. Granville, G. R. Holtom, and B. E. Kohler, *J. Chem. Phys.* **72**, 4671 (1980).
⁴⁰ B. S. Hudson and J. R. Andrews, *Chem. Phys. Lett.* **63**, 493 (1979).
⁴¹ A. C. Lasaga, R. J. Aerni, and M. Karplus, *J. Chem. Phys.* **73**, 5230 (1980); H. Yoshida and M. Tasumi, *ibid.* **89**, 2803 (1988).
⁴² J. Murakami, M. Ito, and K. Kaya, *Chem. Phys. Lett.* **80**, 203 (1981).
⁴³ M. Ito, *J. Phys. Chem.* **91**, 517 (1987).
⁴⁴ M. Ito, T. Ebata, and N. Mikami, *Annu. Rev. Phys. Chem.* **39**, 123 (1988).
⁴⁵ R. J. Poon, J. A. Wozniak, F. P. Bernstein, and J. I. Seaman, *J. Chem. Phys.* **87**, 1917 (1987).
⁴⁶ K. Okuyama, N. Mikami, and M. Ito, *J. Phys. Chem.* **89**, 5617 (1985).
⁴⁷ W. H. Flygare, *Molecular Structure and Dynamics* (Prentice-Hall, Englewood Cliffs, NJ, 1978), pp. 128-135.
⁴⁸ E. Hirota, *J. Chem. Phys.* **45**, 1984 (1966).

- ⁵⁷D. R. Lide, Jr. and M. Jen, *J. Chem. Phys.* **40**, 252 (1964).
⁵⁸S. L. Hsu and W. H. Flygare, *J. Mol. Spectrosc.* **32**, 375 (1969).
⁵⁹U. Dinur, R. J. Hemley, and M. Karplus, *J. Phys. Chem.* **87**, 924 (1983).
⁶⁰R. J. Hemley, B. Brooks, and M. Karplus, *J. Chem. Phys.* **85**, 6550 (1986).
⁶¹R. J. Hemley, A. C. Lasaga, V. Vaida, and M. Karplus, *J. Phys. Chem.* **92**, 945 (1988).
⁶²M. Aoyagi, I. Ohmine, and B. Kohler, *J. Phys. Chem.* **94**, 3922 (1990).
⁶³A. E. Dorigo, D. W. Pratt, and K. N. Houk, *J. Am. Chem. Soc.* **109**, 6591 (1987).
⁶⁴J. R. Andrews and B. S. Hudson, *J. Chem. Phys.* **68**, 4587 (1978).
⁶⁵L. Spangler and D. Pratt, *J. Chem. Phys.* **84**, 4789 (1986).
⁶⁶H. C. Longuet-Higgins, *Mol. Phys.* **6**, 445 (1963).
⁶⁷P. Groner and J. R. Durig, *J. Chem. Phys.* **66**, 1856 (1977).
⁶⁸P. Groner, J. F. Sullivan, and J. R. Durig, *Vibrational Spectra and Structure*, edited by J. R. Durig (Elsevier, New York, 1981), Vol. 9, p. 405.